Available online at www.sciencedirect.com
SCIENCE DIRECT
Polymer 46 (2005) 3767–3775
polymer
www.elsevier.com/locate/polymer

Synthesis and electroluminescent property of poly(*p*-phenylenevinylene)s bearing triarylamine pendants

Fushun Liang[a], Yong-Jin Pu[a], Takashi Kurata[a], Junji Kido[b], Hiroyuki Nishide[a,*]

[a]*Department of Applied Chemistry, Waseda University, Tokyo, 169-8555 Japan*
[b]*Department of Polymer Science and Engineering, Yamagata University, Yonezawa, 992-8510 Japan*

Received 3 November 2004; received in revised form 2 March 2005; accepted 14 March 2005

Abstract

Two poly(*p*-phenylenevinylene) derivatives, TPA-PPV and TPA-CN-PPV, bearing a triarylamine pendant were synthesized by the Wittig-Horner and Knoevenagel reactions, respectively. The optical properties of the polymers were improved by energy transfer from the triarylamine pendant to the poly(*p*-phenylenevinylene) main chain. Cyclic voltammetry revealed that the HOMO energy level of the pendant TPA moiety is higher than that of the PPV main chain, suggesting that the hole injection from ITO into the TPA moiety, then from the TPA moiety into PPV is more favorable than directly from ITO into the PPV main chain. A single-layer light-emitting diode using TPA-PPV as the emitting layer exhibited a maximum brightness of 790 cd/m^2 at a bias of 8 V, while the control device employing commercially available MEH-PPV as the emitter showed a maximum brightness of 250 cd/m^2 under 11 V. The higher brightness combined with the higher current density was attributed to the effective hole injection and/or hole transport in the TPA-PPV-based device.
© 2005 Elsevier Ltd. All rights reserved.

Keywords: Polymer materials; Electroluminescence; Hole injection and transport

1. Introduction

Light-emitting diodes (LEDs) have attracted considerable attention due to their potential application in flat-panel displays [1–3]. Especially, for large-area displays, polymer materials have been an important candidate as an emitting material because of their wet-processable ability by a spin-coating or ink-jetting method. The following three issues have been considered to be essential for the polymeric emitting polymers: (i) high photoluminescent (PL) efficiency in a homogeneous solution, (ii) no significant intermolecular aggregation in the solid state, and (iii) good charge-carrier injecting and transporting capability upon assembling into an electroluminescent (EL) device [4].

Poly(*p*-phenylenevinylene)s (PPVs), as one kind of π-conjugated polymer, are ideal candidates for electroluminescence, because they exhibit high PL efficiency in solution, and do not significantly aggregate in the solid state. PPVs possess a hole transport capability, however, the hole mobility, around 10^{-6} to 10^{-7} cm^2/Vs, is not high enough to satisfy the need for effective hole injection and transporting in light-emitting devices [5,6]. This should have some influence on the electroluminescent efficiency. The triphenylamine derivative (TPA) is well known as a typical hole-transporting material and has a hole mobility of 10^{-3} to 10^{-5} cm^2/Vs [7,8]. We assume in this paper that the incorporation of a TPA moiety into the PPV backbone improves the hole mobility of PPV. Besides that the hole injecting and transporting ability of PPV could be improved, there are two additional advantages upon the incorporation of a TPA moiety into PPV. First, a self-quenching of excitons caused by the intermolecular interaction would be reduced because TPA is characterized as a tri-dimensional steric group. Second, an energy transfer from the TPA moiety to the PPV backbone is expected because TPA may act as a UV-light harvesting group.

There have been several reports on the improvement of π-conjugated polymers such as PPV and polyfluorene by introducing hole-transporting and/or electron-transporting groups to realize highly efficient electroluminescence [9–17]. For example, Jin et al. reported PPV-based copolymers containing an oxadiazole group with an electron injecting

* Corresponding author. Tel.: +81 3 3200 2669; fax: +81 3 3209 5522.
E-mail address: nishide@waseda.jp (H. Nishide).

0032-3861/$ - see front matter © 2005 Elsevier Ltd. All rights reserved.
doi:10.1016/j.polymer.2005.03.036

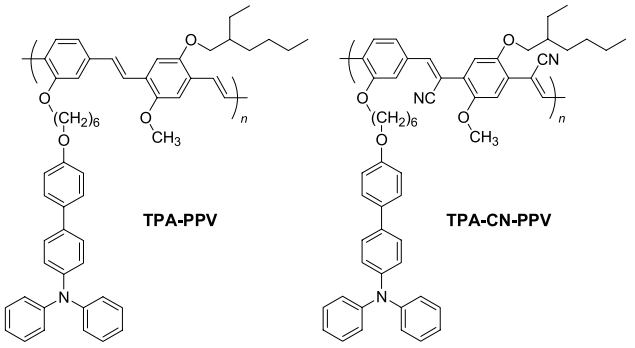

Scheme 1.

and transporting ability [9]. Müllen et al. reported a TPA-substituted polyfluorene, towards improved hole injection for LEDs [10]. A highly efficient blue-light-emitting fluorene copolymer with the hole-transporting TPA and the electron-transporting oxadiazole pendant group was synthesized by Shu et al. in which the bipolar substituents provide both functions of simultaneously suppressing the aggregation and improving the charge injection [11].

Recently, we reported TPA-substituted PPVs in which TPA was introduced into the PPV main chain or directly attached to the PPV backbone [18–21]. We extended the design by synthesizing a structure in which the TPA moiety is combined with the PPV main chain with a spacer group (see Scheme 1 for the structures). The functional TPA moiety and the PPV main chain are anticipated to retain their own hole-transporting and emitting property, respectively. In addition, the TPA substituent performs the function of solubilizing, suppressing the aggregation, and energy transfer. The TPA moiety was linked with the PPV backbone by a 6-C alkoxy chain through multiple-step synthesis. To our best knowledge, this is the first report on electroluminescent PPVs incorporating TPA as a side chain by a flexible linkage. The experimental results indicate that the as-synthesized PPV polymer bearing the TPA pendent showed higher brightness and EL efficiency, which are superior to those of the commercially available MEH-PPV.

2. Experimental section

2.1. Characterization

The ^{1}H NMR and ^{13}C NMR spectra were recorded at room temperature on a Lambda 500 spectrometer and deuterated chloroform and tetramethylsilane (TMS) were used as the internal standard. The mass spectra were measured on a Shimadzu GCMS-QP5050 instrument. Thermal analyses were performed using SEIKO DSC220C and TG/DTA220 thermal analyzers at a heating rate of 10 °C/min under nitrogen. Gel permeation chromatography (GPC) was performed with $CHCl_3$ as an eluent and polystyrene as a standard using a TOSOH LS-8000 instrument. The UV–vis and photoluminescent spectra were recorded on a JASCO V-500 and a Hitachi F-4500 spectrometer, respectively. Cyclic voltammetry (CV) was conducted using a CV-50W Voltammetric Analyzer, BAS with a typical three-electrode cell with a solution of Bu_4NBF_4 (0.1 M) in acetonitrile at a scan rate of 20 mV/s. The polymer films were spin-coated on ITO glasses and then dried in air. A Pt wire was used as the counter electrode, and a Ag/AgCl electrode was used as the reference electrode. Prior to each series of measurements, the cell was deoxygenated with argon.

2.2. Materials

2,5-Xylenol, 4-bromophenol, triphenylamine, tri-*i*-propylborate, potassium *tert*-butoxide, triethyl phosphate, 1,6-dibromohexane, 2,2′-azobis-(2-methylpropionitrile), pyridinium chlorochromate, *n*-butyllithium (1.6 M in hexane), tetrakis(triphenylphosphine) palladium, paraformaldehyde, and HBr (30 wt% in acetic acid) were purchased from Tokyo Kasei Co. and Kanto Chemical Co. and used without further purification. MEH-PPV was purchased from Aldrich Chemical Co.

2.3. Synthesis

2.3.1. 2-(6-Bromohexyloxy)-1,4-dimethylbenzene (*1*)

A solution of 1,6-dibromohexane (146 g, 0.60 mol) in ethanol (100 mL) was added dropwise into a mixture of 2,5-xylenol (12.2 g, 0.10 mol), KOH (8.42 g, 0.15 mol), and ethanol (150 mL), and then the mixture was refluxed for 24 h. After cooling, the solvent was evaporated, and the residue was dissolved in ether and washed with 1 N HCl and water. The excess 1,6-dibromohexane was removed in vacuum to give a colorless oil (25.1 g, 88%). ^{1}H NMR ($CDCl_3$, 500 MHz; ppm) δ 6.99 (d, $J=7.5$ Hz, 1H), 6.64 (t, $J=7.5$ Hz, 2H), 3.93 (t, $J=6.4$ Hz, 2H), 3.41 (t, $J=6.7$ Hz, 2H), 2.31 (s, 3H), 2.17 (s, 3H), 1.84 (m, 4H), 1.52 (s, 4H); ^{13}C NMR ($CDCl_3$, 125 MHz; ppm) δ 157.00, 136.40, 130.27, 123.57, 120.64, 111.97, 67.55, 33.71, 32.49, 29.21, 27.92, 25.38, 21.37, 15.76; MS (EI) *m/e* 284 $[(M-1)^+]$, 286 $[(M+1)^+]$, 285.08 (calcd). Anal. Calcd for $C_{14}H_{21}BrO$: C, 59.0; H, 7.4. Found: C, 59.1; H, 7.6.

2.3.2. 2-(6-(p-Bromophenoxy)hexyloxy)-1,4-dimethylbenzene (*2*)

A mixture of **1** (11.40 g, 40 mmol), *p*-bromophenol (6.92 g, 40 mmol), sodium hydroxide (11.06 g, 80 mmol), and DMF (150 mL) was stirred and heated to 80 °C for 24 h. It was subsequently poured into ice water (500 mL). The resulting solid was collected by filtration and then recrystallized from a mixture of ethanol and dichloromethane to give white crystals (14.0 g, 93%). mp: 75–77 °C. ^{1}H NMR ($CDCl_3$, 500 MHz; ppm) δ 7.36 (m, 2H), 7.01 (t, $J=6.7$ Hz, 1H), 6.77 (m, 2H), 6.64 (t, $J=6.9$ Hz, 1H), 6.63 (d, $J=5.5$ Hz, 1H), 3.95 (s, 4H), 2.31 (s, 3H), 2.17 (s, 3H),

1.82 (s, 4H), 1.55 (s, 4H); ^{13}C NMR ($CDCl_3$, 125 MHz; ppm) δ 158.22, 157.06, 136.45, 132.19, 130.30, 123.62, 120.64, 116.31, 112.62, 112.01, 68.13, 67.65, 29.33, 25.96, 21.40, 15.77; MS (EI) *m/e* 376 [$(M-1)^+$], 378 [$(M+1)^+$], 377.11 (calcd). Anal. Calcd for $C_{20}H_{25}BrO_2$: C, 63.7; H, 6.7. Found: C, 63.6; H, 6.8.

2.3.3. 2-(6-(p-Bromophenoxy)hexyloxy)-1,4-bis(hydroxymethyl)benzene (**3**)

A solution of **2** (4.0 g, 10.6 mmol), *N*-bromosuccinimide (3.96 g, 22.3 mmol), and a small amount of 2,2′-azobis-(2-methylpropionitrile) in carbon tetrachloride (300 L) was heated at reflux for 3 h. After cooling, the solution was filtered and the solvent was removed to give a pale yellow oil containing a mixture of brominated products. A mixture of the crude residue and anhydrous sodium acetate (5.2 g, 63.6 mmol) in acetic anhydride (100 mL) was heated at reflux for overnight. After cooling, the solvent was removed to give a brown oil containing a mixture of acetylated products. A mixture of the crude residue, methanol (160 mL), and aqueous sodium hydroxide (4 g dissolved in 24 mL water) was heated at reflux for 2 h. After cooling, the solvent was removed and chloroform was added. The organic layer was washed with water, dried and filtered. The residue was purified with chromatography on a silica gel column with chloroform as an eluent to give a yellow solid (1.52 g, 35%). mp: 81–83 °C. ^{1}H NMR ($CDCl_3$, 500 MHz; ppm) δ 7.36 (d, $J=9.0$ Hz, 2H), 7.25 (t, $J=7.8$ Hz, 1H), 6.91 (t, $J=6.4$ Hz, 2H), 6.76 (d, $J=9.0$ Hz, 2H), 4.68 (s, 2H), 4.67 (s, 2H), 4.05 (t, $J=6.5$ Hz, 2H), 3.93 (t, $J=6.4$ Hz, 2H), 2.27 (s, 1H), 1.85 (t, $J=6.5$ Hz, 2H), 1.81 (t, $J=6.5$ Hz, 2H), 1.63 (t, 1H), 1.54 (s, 4H); ^{13}C NMR ($CDCl_3$, 125 MHz; ppm) δ 158.17, 156.36, 141.98, 132.20, 128.77, 128.58, 118.83, 116.30, 112.66, 109.72, 68.02, 67.87, 65.27, 62.05, 29.19, 29.10, 25.94, 25.80; MS (LRFAB) *m/e* 408 [$(M-1)^+$], 410 [$(M+1)^+$], 409.31 (calcd). Anal. Calcd for $C_{20}H_{25}BrO_4$: C, 58.7; H, 6.2. Found: C, 58.9; H, 6.2.

2.3.4. 2-(6′-p-Bromophenoxy)hexyloxyterephthalaldehyde (**4**)

A stirred suspension of **3** (2.0 g, 4.88 mmol) and PCC (3.24 g, 14.7 mmol) in dichloromethane (50 mL, 0.11 M) was heated at reflux for 2 h. After cooling, the black precipitate was filtered off and the solution was concentrated. The crude product was purified by chromatography on a silica gel with dichloromethane as an eluent. The product was recrystallized from hexane to give a white crystal (1.7 g, 80%). mp: 84–86 °C. ^{1}H NMR ($CDCl_3$, 500 MHz; ppm) δ 10.56 (s, 1H), 10.04 (s, 1H), 7.98 (s, 1H), 7.50 (d, $J=8.25$ Hz, 2H), 7.36 (s, 2H), 7.34 (s, 1H), 6.77 (d, $J=8.4$ Hz, 2H), 4.18 (t, $J=6.4$ Hz, 2H), 3.94 (t, $J=6.4$ Hz, 2H), 1.92 (t, $J=6.6$ Hz, 2H), 1.82 (t, $J=6.6$ Hz, 2H), 1.57 (s, 4H); ^{13}C NMR ($CDCl_3$, 125 MHz; ppm) δ 191.49, 189.31, 161.46, 158.13, 141.34, 132.22, 129.08, 128.47, 123.01, 116.27, 112.67, 111.47, 68.83, 67.95, 29.08, 28.88, 25.80, 25.77; MS (LRFAB) *m/e* 404 [$(M-1)^+$], 406 [$(M+1)^+$], 405.28 (calcd). Anal. Calcd for $C_{20}H_{21}BrO_4$: C, 59.3; H, 5.2. Found: C, 59.3; H, 5.3.

2.3.5. N-(4-Bromophenyl)-N,N-diphenylamine (**5**)

A solution of triphenylamine (3.00 g, 12.2 mmol) and *N*-bromosuccinimide (2.14 g, 12.0 mmol, 0.98 equiv) in carbon tetrachloride (31.0 mL, 0.39 M) was heated at 50 °C for 9 h under nitrogen atmosphere. After cooling, the solution was filtered and the solvent was evaporated. The crude residue was recrystallized from hexane and dichloromethane to give a white crystal (2.35 g, 59%). mp: 110–112 °C. ^{1}H NMR ($CDCl_3$, 500 MHz; ppm) δ 7.32 (d, $J=8.4$ Hz, 2H), 7.27–7.23 (m, 4H), 7.07 (d, $J=8.0$ Hz, 4H), 7.03 (t, 2H), 6.94 (d, $J=8.4$ Hz, 2H); ^{13}C NMR ($CDCl_3$, 125 MHz; ppm) δ 147.4, 147.0, 132.1, 129.4, 125.1, 124.4, 123.2, 114.8; MS (EI) *m/e* 323 [$(M-1)^+$], 325 [$(M+1)^+$], 324.2 (calcd). Anal. Calcd for $C_{18}H_{14}BrN$: C, 66.7; H, 4.4; N, 4.3. Found: C, 66.8; H, 4.4; N, 4.2.

2.3.6. Pinacol(4-(N, N-diphenylamino)-1-phenyl)boronate (**6**)

n-Butyllithium (10.6 mL, 17.0 mmol, 1.6 M in hexane) was added dropwise to **5** (5.01 g, 15.4 mmol) in a dried THF (154 mL, 0.1 M) at −78 °C and stirred for 15 min. The mixture was then transferred via teflon tube into a solution of tri-*i*-propylborate (14.5 g, 77.1 mmol, 5.0 equiv) in a dried THF (38.5 mL, 2.0 M) at −78 °C and the reaction mixture was stirred for 2 h. After the mixture was allowed to warm to room temperature, pinacol was added and the mixture stirred overnight. The solvent was evaporated and the residue was dissolved in hexane/dichloromethane (2/1) and filtered. The crude product was purified by flash chromatography on the deactivated silica gel with triethylamine with hexane/dichloromethane (10/1) as an eluent to give a colorless oil (4.7 g, 82%). ^{1}H NMR ($CDCl_3$, 500 MHz; ppm) δ 7.66 (d, $J=8.4$ Hz, 2H), 7.24 (d, $J=8.25$ Hz, 4H), 7.10 (d, $J=8.25$ Hz, 4H), 7.04 (t, 2H), 7.02 (d, $J=8.4$ Hz, 2H), 1.33 (s, 12H); ^{13}C NMR ($CDCl_3$, 125 MHz; ppm) δ 150.59, 147.40, 135.84, 129.28, 124.98, 123.34, 121.80, 83.55, 24.85; MS (LRFAB) *m/e* 371 [M^+], 371.21 (calcd). Anal. Calcd for $C_{24}H_{26}BNO_2$: C, 77.6; H, 7.1; N, 3.8. Found: C, 77.4; H, 7.3; N, 3.8.

2.3.7. 2-[6-(p-(N, N-diphenylamino)biphenyloxy)hexyloxy]terephthalaldehyde (**7**)

To a DMF (10.0 mL) solution of **4** (0.405 g, 1.0 mmol), **6** (0.408 g, 1.1 mmol), and K_3PO_4 (0.32 g, 1.5 mmol) was added $Pd(PPh_3)_4$ (0.024 g, 0.02 mmol) at 60 °C under nitrogen. The mixture was stirred at 100 °C for 15 h and then extracted with dichloromethane. The organic layer was washed with water, dried over anhydrous sodium sulfate, filtered and evaporated. The crude product was purified using a silica gel column with a hexane/dichloromethane (4/1) eluent. Recrystalization from hexane gave monomer **7** (0.42 g, 74%). mp: 118–120 °C. ^{1}H NMR ($CDCl_3$,

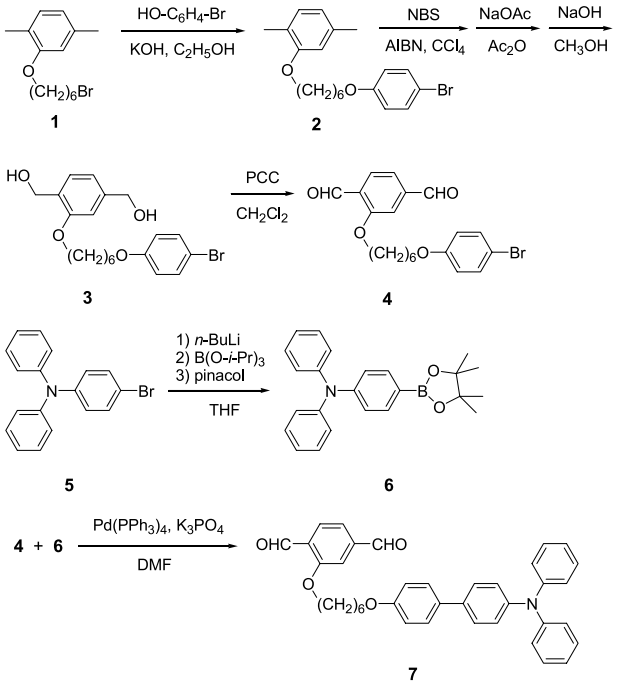

Scheme 2.

500 MHz; ppm) δ 10.57 (s, 1H), 10.04 (s, 1H), 7.98 (d, $J=$ 8.0 Hz, 1H), 7.50–7.47, (m, 4H), 7.41 (d, $J=8.9$ Hz, 2H), 7.25 (t, $J=6.7$ Hz, 4H), 7.11 (m, 6H), 7.01 (t, $J=7.4$ Hz, 2H), 6.93 (d, $J=8.9$ Hz, 2H), 4.19 (t, $J=6.4$ Hz, 2H), 4.01 (t, $J=6.4$ Hz, 2H), 1.94 (t, 2H), 1.85 (t, 2H), 1.57 (s, 4H); ^{13}C NMR ($CDCl_3$, 125 MHz; ppm) δ 191.47, 189.31, 161.47, 158.27, 147.75, 146.55, 141.32, 135.00, 133.15, 129.20, 129.04, 128.67, 127.63, 127.28, 124.20, 122.91, 122.72, 114.74, 111.56, 68.86, 67.76, 29.19, 28.90, 25.83, 25.81; MS (EI) *m/e* 569, 569.69 (calcd). Anal. Calcd for $C_{38}H_{35}NO_4$: C, 80.1; H, 6.2; N, 2.5. Found: C, 79.9; H, 6.3; N, 2.5.

2.3.8. Preparation of TPA-PPV

To a xylene (6.0 mL) solution of **7** (0.285 g, 0.5 mmol) and **8** (0.268 g, 0.5 mmol) was added solid potassium *tert*-butoxide (0.168 g, 1.5 mmol) at 60 °C. The solution was stirred at 100 °C for 5 h under nitrogen. The reaction mixture was extracted with chloroform. The organic layer was washed with water, dried over anhydrous sodium sulfate, filtered and evaporated. The polymer dissolved in a minimum amount of chloroform was precipitated into methanol to give a bright orange powder (0.261 g, 66%). ^{1}H NMR ($CDCl_3$, 500 MHz; ppm) δ 7.60–6.75 (m, 27H), 4.12–3.81 (m, 9H), 1.95–1.23 (m, 17H), 0.92 (overlapping, broad s, 6H); ^{13}C NMR ($CDCl_3$, 125 MHz; ppm) δ 158.31, 156.63, 151.46, 147.75, 146.52, 138.23, 135.07, 133.05, 129.64, 129.21, 127.62, 127.29, 126.99, 126.40, 126.05, 124.21, 123.92, 122.72, 119.53, 114.72, 110.38, 109.79, 108.91, 71.79, 68.28, 67.86, 61.92, 56.37, 39.74, 30.98, 29.29, 25.95, 24.33, 24.17, 23.12, 16.39, 14.14, 11.47, 11.28.

2.3.9. Preparation of TPA-CN-PPV

To a solution of 0.2223 g (0.4733 mmol) of **7** and 0.1487 g (0.4733 mmol) of **9** in 4 mL of THF and 1 mL of MeOH at reflux under nitrogen was added 0.23 mL of Bu_4NOH in methanol (1 M). After refluxing for 40 min, the reaction mixture was poured into MeOH (50 mL), and the precipitate was collected by filtration. The polymer dissolved in a minimum amount of $CHCl_3$ was precipitated into methanol to give a bright orange powder (0.268 g, 74%). ^{1}H NMR ($CDCl_3$, 500 MHz; ppm) δ 8.28–7.41, 7.25–6.72 (m, 25 H), 4.17–3.70 (m, 9H), 2.17–1.29 (m, 17H), 0.91 (overlapping s, 6H); ^{13}C NMR ($CDCl_3$, 125 MHz; ppm) δ 161.35, 158.25, 158.09, 151.03, 150.48, 147.75, 146.55, 141.16, 140.70, 135.06, 134.94, 133.14, 132.20, 129.23, 128.67, 127.64, 127.28, 124.22, 122.74, 118.04, 117.47, 116.32, 116.23, 114.76, 114.71, 112.66, 111.95, 110.63, 71.94, 68.70, 67.94, 67.84, 56.60, 39.51, 30.64, 29.70, 25.86, 24.02, 23.01, 22.96, 19.71, 17.66, 14.08, 11.22.

2.4. Device fabrication and testing

The EL devices were fabricated on indium tin oxide (ITO) substrates that have been ultrasonicated sequentially in detergent, methanol, 2-propanol, and acetone and have been treated with O_2 plasma for 10 min under UV light before use. A hole-injecting layer, PEDOT was spin-coated at a spin rate of 1550 rpm from its water solution (1.3 wt%) onto the ITO substrates and annealed at 110 °C for 60 min under vacuum. The emissive layers were prepared by spin-casting from the solution in chloroform (10 mg/mL, 2500 rpm) and then annealed at 80 °C for 60 min under vacuum. Prior to spin-coating, the polymer solution was filtered using a 0.45 μm membrane filter. The metal electrodes Ca and Al were deposited onto the surface of the spin-coated polymer film by thermal evaporation technique at 10^{-6} Torr through a shadow mask. The typical active area of the LEDs was 5 mm^2. The EL spectra were measured on a Hamamatsu photonic multi-channel analyzer. The current–voltage (*I–V*) characteristics and luminance were measured using a Keithley 2400 Source Meter and a TOPCON BM-8, respectively.

3. Results and discussion

3.1. Synthesis and characterization

The synthetic routes of the monomers and the corresponding polymers are shown in Schemes 1 and 2, respectively. The key monomer for the synthesis of the target polymers is the triphenylamine containing dialdehyde monomer **7**, which was prepared by Suzuki coupling of the 2-(6′-*p*-bromophenoxyalkoxy)terephthalaldehyde **4** and the pinacol(diphenylamino-phenyl)boronate **6**. In our experiment, compound **6** is an important intermediate, which was

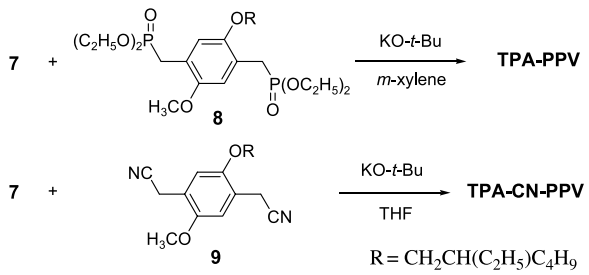

Scheme 3.

conducted through two steps [19]. First, monobromotriphenylamine **5** was selectively obtained using 1 equiv of *N*-bromosuccinimide. Second, the di-*i*-propyl borate ester was prepared by the lithiation of **5** and then the di-*i*-propyl borate ester was exchanged to pinacol borate ester **6**. Compound **6** was stable for column chromatography on deactivated silica gel pretreated with triethylamine. 1-(6′-*p*-Bromophenoxy)hexyloxy-2,5-dimethylbenzene **2** was easily obtained by two steps Williamson ether synthesis in high yield. Bisbenzylalcohol **3** was synthesized by the benzybromination, esterification, and hydrolysis of **2**. Subsequently, **3** was oxidized by pyridinium chlorochromate (PCC) to afford the terephthalaldehyde **4**. The xylene-bis(diethylphosphonate) monomer **8** was quantitatively prepared by the Arbuzov reaction of the corresponding α,α-dibromoxylene [22,23]. The bismethylene nitrile monomer **9** was prepared by the treatment of α,α-dichloroxylene with NaCN in DMF solution (Scheme 3) [24,25].

The Wittig-Horner type polymerization of **7** and **8** was carried out in a *m*-xylene solution in the presence of potassium *tert*-butoxide at 110 °C. TPA-PPV was obtained as a bright orange powder in over 66% yield. A TPA-containing CN-PPV was also synthesized using the Knoevenagel polymerization reaction, with the purpose of improving the electron affinity of the PPV main chain by introduction of a strong electron-withdrawing CN group to the double bond of PPV. This reaction was carried out between monomers **7** and **9** in a THF solution at 50 °C in the presence of potassium *tert*-butoxide. The polymers were easily soluble in common organic solvents, such as chloroform, toluene, and tetrahydrofuran.

The molecular structures of the monomers and the corresponding polymers were identified by ^{1}H NMR, ^{13}C NMR, and elemental analysis. The ^{1}H NMR spectra of **7** and the polymers were shown in Fig. 1. By comparison we can see that the proton signal peaks from the dialdehyde monomer **7** ($\delta = 10.57$, 10.04 ppm) disappear in polymer TPA-PPV and TPA-CN-PPV, indicating the complete polymerization. Simultaneously, there were no significant peaks at around 6.5 ppm, which is assigned to the proton signals from *cis*-vinylene double bond, suggests the formation of dominant *trans*-configuration in the vinylene double bonds among the polymers.

Table 1 summarizes the polymerization results, molecular weights, and thermal data. The molecular weights were determined by gel permeation chromatography (GPC) using polystyrene as the standard. The weight average molecular

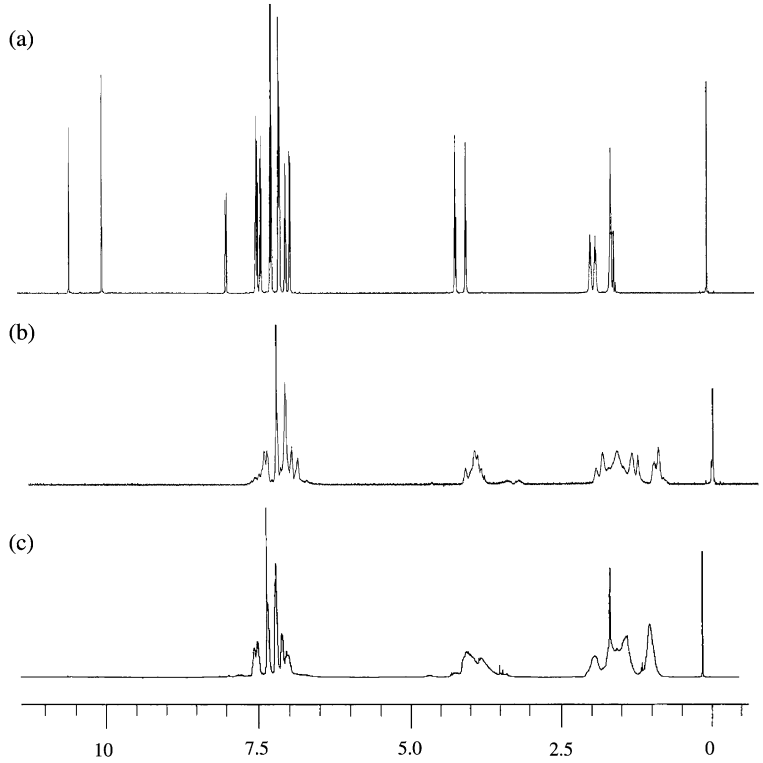

Fig. 1. The ^{1}H NMR spectra of the monomer 7 (a), the polymer TPA-PPV (b), and TPA-CN-PPV (c) in the $CDCl_3$ solution.

Table 1
Molecular weight, thermal and optical properties of the polymers

Polymers	M_w[a]	M_w/M_n[a]	T_d[b] (°C)	T_g[c] (°C)	Abs (film) (nm)	PL (film) (nm)
TPA-PPV	11,800	1.20	389	148	326, 471	551
TPA-CN-PPV	20,800	1.27	367	137	321, 400	560

[a] Determined by GPC in $CHCl_3$ based on polystyrene standards.
[b] Temperature at 5% weight loss under nitrogen.
[c] Determined by DSC at a heating rate of 10 °C/min under nitrogen.

weight (M_w) and polydispersity of the polymers were found to be 11,800, 1.20 and 20,800, 1.27, respectively. The thermal properties of the polymers were determined by DSC and TGA (heating at 10 °C/min in nitrogen) measurements. Both TPA-PPV and TPA-CN-PPV showed a high thermal stability with a 5% weight loss at 389 and 367 °C, respectively.

3.2. Optical properties

Fig. 2 shows the absorption and photoluminescent spectra of TPA-PPV and TPA-CN-PPV in $CHCl_3$ solution and as solid film, respectively. The polymer TPA-PPV exhibits two absorption bands at around 324 and 456 nm in $CHCl_3$ solution and around 326 and 471 nm in the solid film. The high energy bands (324 and 326 nm) are attributed to the absorption of the TPA segment. The 456 nm peak in solution and the 471 nm peak in the solid film are associated with the absorption of the π-conjugated PPV main chain. A similar trend was observed for the absorption of polymer TPA-CN-PPV. The detailed data were listed in Table 1.

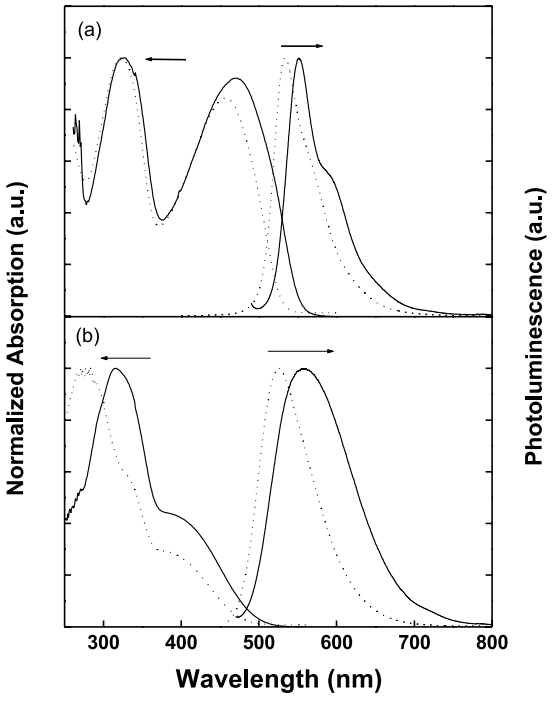

Fig. 2. UV–vis and photoluminescent spectra of TPA-PPV (a) and TPA-CN-PPV (b) in the $CHCl_3$ solution (dotted lines) and in the film state (solid lines).

TPA-PPV shows an emission maximum at 551 nm and a shoulder peak at 592 nm in the solid film state, about 18 nm red-shifted relative to the emission in dilute solution (533 nm). It should be noted that same photoluminescent emission maximum was observed irrespective of excitation at 326 or 471 nm. This indicates the existence of an intramolecular energy transfer from the TPA segment to the PPV main chain. This is helpful for improving the PL efficiency. TPA-CN-PPV exhibits a single structureless and broad emission peak both in solution (centered at 524 nm) and in the solid film (centered at 560 nm), with a red shift of 36 nm. The half maximum wavelength of the film spectrum of TPA-CN-PPV is 113 nm, which is significantly broader than that of TPA-PPV (66 nm).

3.3. Electrochemical properties

The electrochemical behavior of the polymers was investigated by cyclic voltammetry (CV). The polymer films deposited on ITO glass were scanned both positively and negatively separately in 0.10 M of anhydrous acetonitrile solution of *n*-$BuNBF_4$ against Ag/AgCl calibrated with ferrocene (Fc/Fc^+). From Fig. 3 we can see that upon the anodic scan, TPA-PPV exhibits two well-separated reversible oxidation peaks, which means the existence of two oxidation steps. The first oxidation potential peak with an onset value at 1.03 V is attributed to the *p*-doping of the TPA segments. The second oxidation peak with an onset value at around 1.27 V is assigned to the PPV main chain. Upon the cathodic scan, a reduction peak with an onset potential at −1.17 V was observed, which corresponds to

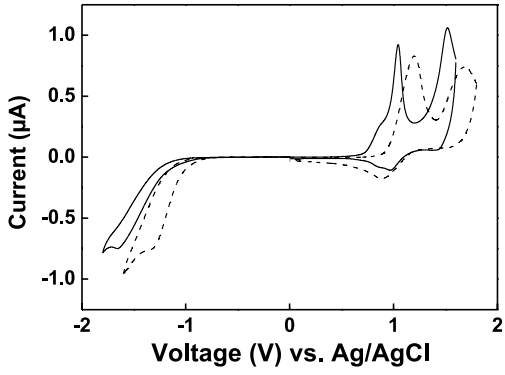

Fig. 3. Cyclic voltammogram of TPA-PPV (solid line) and TPA-CN-PPV (dashed line) film coated on an ITO glass, measured in 0.1 M acetonitrile solution of $(C_4H_9)_4NBF_4$.

Table 2
Oxidation and reduction potentials (E_{ox} and E_{red}) of the polymers

Polymers	E_{red} (V)	E_{ox} (V)	HOMO (eV)	LUMO (eV)	E_g[a] (eV)
TPA-PPV	−1.17	1.03	−5.43	−3.23	2.20
		1.27	−5.67		2.44
TPA-CN-PPV	−1.03	0.99	−5.39	−3.37	2.02
		1.34	−5.74		2.37

[a] The E_g value is calculated from oxidation and reduction potential.

the reduction process of the PPV main chain. The onset of the oxidation process for TPA-CN-PPV occurs at 0.99 V, derived from the TPA segment and 1.34 V, derived from the CN-PPV main chain. The reduction onset potential is −1.03 V, which is attributed from CN groups attached with vinylene double bonds. Table 2 summarizes the oxidation and reduction potentials derived from the onset. The HOMO and LUMO levels calculated according to an empirical formula ($E_{HOMO} = -(E_{ox}^{onset} + 4.4)$ eV and $E_{LUMO} = -(E_{red}^{onset} + 4.4)$ eV) are also listed in Table 2 [26,27]. The HOMO and LUMO of the polymers were estimated to be −5.43 (−5.67), −5.39 (−5.74) and −3.32, −3.37, respectively. Because the HOMO energy level of TPA is higher than that of PPV main chain, the injection of holes into the HOMO of TPA in TPA-PPV is more favorable than directly into that of PPV [28]. Hence it is concluded from the HOMO energy levels that the hole injection from ITO (−4.8–5.0 eV) into PPV backbone can be improved due to the incorporation of the TPA functional groups.

3.4. Electroluminescent properties

In order to investigate the electroluminescent performance, devices from polymer TPA-PPV were fabricated with the configuration of ITO/TPA-PPV (100 nm)/Ca/Al. From the device a bright yellow light was observed and the EL spectrum (solid line) was shown in Fig. 4. The maximum emission wavelength is located at 551 nm with a shoulder peak at 592 nm. It was found that the EL spectrum is nearly identical to its PL spectrum of TPA-PPV in the film state. This indicates that the EL and PL behaviors originated from the same excited state. For comparison purposes, a control device with the structure of ITO/MEH-PPV (100 nm)/Ca/Al and a blend device with the structure of ITO/TPA:MEH-PPV (100 nm)/Ca/Al were constructed under the same condition. In the latter 47 wt% of TPA was physically blended into MEH-PPV. Fig. 5(a) and (b) showed the current–voltage (*I–V*) curves and luminance–voltage (*L–V*) curves, respectively. From it one can see that the turn-on voltage decreased gradually from 5.5 V (control device) to 3.5 V (blend device) to 3 V (TPA-PPV device). The control MEH-PPV device gave a maximum luminance of 250 cd/m^2 at a bias of 11 V. Upon physical blending between TPA and MEH-PPV, the maximum luminance was 520 cd/m^2 at 10 V. Both the current and power efficiency increased. After chemical modification, by which we introduced TPA into PPV, the device performance was significantly improved. The maximum brightness was 790 cd/m^2 at a bias of 7.5 V. The maximum power efficiency of TPA-PPV was 4.4 times higher than that of MEH-PPV (Table 3). The higher

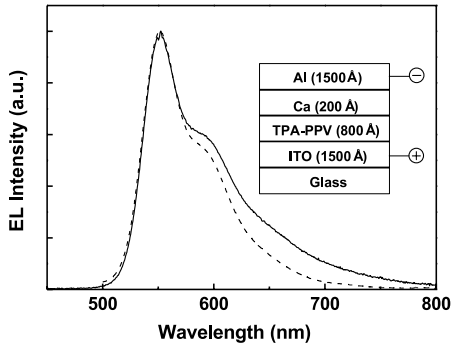

Fig. 4. Electroluminescent spectrum of the device ITO/TPA-PPV/Ca/Al (solid line) and the photoluminescent spectrum of TPA-PPV in the film state (dashed line). (Insert: the single-layer LED structure of TPA-PPV).

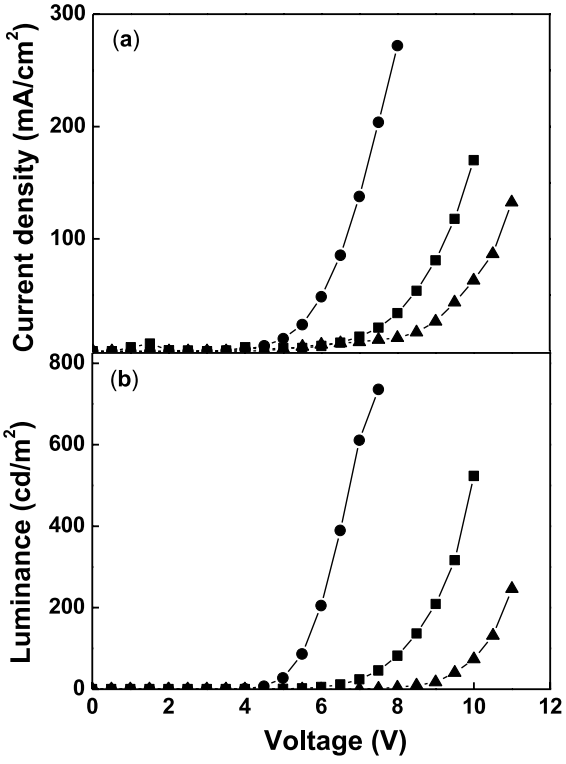

Fig. 5. Current–voltage curves (a) and luminance–voltage curves (b) for the MEH-PPV (▲), the blend of TPA and MEH-PPV (■), and the TPA-PPV (●) in the device configuration of ITO/polymer/Ca/Al.

Table 3
Electroluminescent performance of MEH-PPV and TPA-PPV

Device configuration	Turn-on voltage (V)	Max. brightness (cd/m^2)	Max. current efficiency (cd/A)	Max. power efficiency (lm/W)
ITO/MEH-PPV/Ca/Al	5.5	250 (11 V)	0.19	0.05
ITO/MEH-PPV:TPA/Ca/Al	3.5	520 (10 V)	0.31	0.10
ITO/TPA-PPV/Ca/Al	3	790 (8 V)	0.46	0.22
ITO/PEDOT/TPA-PPV/Ca/Al	2	6190 (7 V)	1.02	0.43

luminance and power efficiency of TPA-PPV combined with the higher current density is attributed to the easier hole injection from the ITO electrode to the HOMO energy level of the TPA moiety and/or better hole transport. Double-layer devices with the configuration of ITO/PEDOT (60 nm)/TPA-PPV (80 nm)/Ca/Al were also fabricated, in which the PEDOT is poly(3,4-ethylenedioxythiophene) doped with poly(styrenesulfonic acid). It exhibited a pronounced enhancement in performance compared with the corresponding single-layer device. The turn-on voltage was as low as 2 V. The maximum brightness reached up to 6190 cd/m^2 at a bias of merely 7 V (Fig. 6). The maximum current efficiency was 1.02 cd/A and the maximum power efficiency was estimated to be 0.43 lm/W. The electroluminescent results indicate that the incorporation of TPA functional groups to light-emitting PPVs is beneficial towards enhancing the device luminance and efficiency due to the improvement in hole-injection and/or transport capability.

To investigate the hole-transporting property of TPA-PPV, a device with the configuration of ITO/TPA-PPV(50 nm)/AlQ (60 nm)/LiF (1 nm)/Al was fabricated. From this device a bright green light was observed, indicating the emission originated from the AlQ layer. The current–voltage–luminance curves were shown in Fig. 7. The result indicated that TPA-PPV could function as a polymeric hole transporting material used in organic LEDs.

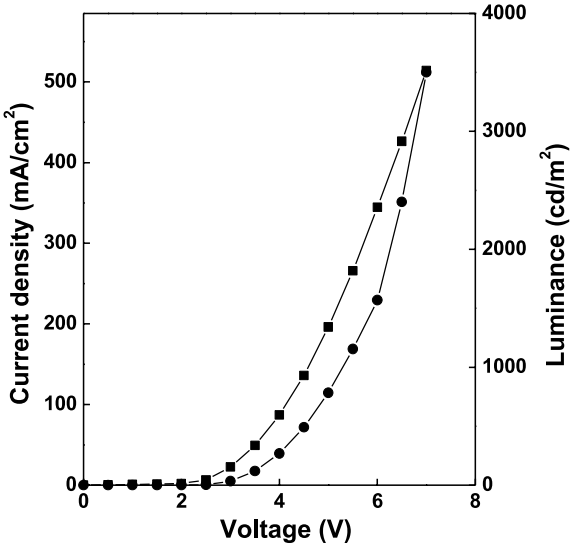

Fig. 6. Current–voltage (■) and luminance–voltage (●) curves for the TPA-PPV in the device configuration of ITO/PEDOT/TPA-PPV/Ca/Al.

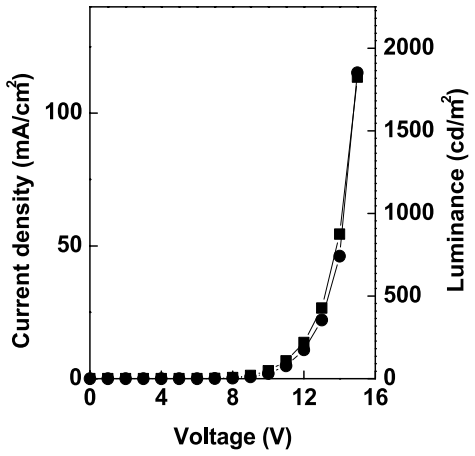

Fig. 7. Current–voltage (■) and luminance–voltage (●) curves for the TPA-PPV in the configuration of ITO/TPA-PPV(50 nm)/AlQ (60 nm)/LiF (1 nm)/Al.

4. Conclusions

We have synthesized two new poly(*p*-phenylenevinylene)s with hole-transporting triarylamine groups as side chains by a multiple-step synthetic procedure. The polymers show an improved hole injection and transport capability over the standard MEH-PPV, thus leading to an increase in device brightness and efficiency. Our results demonstrate that the introduction of hole-transporting functional groups into the PPVs is an effective way to enhance the electroluminescent performance.

Acknowledgements

F. Liang thanks the Postdoctoral Fellowship of the Japan Society for the Promotion of Science (JSPS) for foreign researchers.

References

[1] Burroughes JH, Bradley DDC, Brown AR, Marks RN, Mackay K, Friend RH, et al. Nature 1990;347:539.

[2] Bernius MT, Inbasekaran M, O'Brien J, Wu W. Adv Mater 2000;12: 1737.
[3] Kraft A, Grimsdale AC, Holmes AB. Angew Chem Int Ed 1998;37: 402.
[4] Sun RG, Wang YZ, Wang DK, Zheng QB, Epstein AJ. Synth Met 2000;111–112:403.
[5] Campbell IH, Smith DL, Neff CJ, Ferraris JP. Appl Phys Lett 1999;74: 2809.
[6] Bozano L, Carter SA, Scott JC, Malliaras GG, Brock PJ. Appl Phys Lett 1999;74:1132.
[7] Stolka M, Yanus JF, Pai DM. J Phys Chem 1984;88:4707.
[8] Staudigel J, Stössel M, Steuber F, Simmerer JJ. Appl Phys 1999;86: 3895.
[9] Jin SH, Kim MY, Kim JY, Lee K, Gal YS. J Am Chem Soc 2004;126: 2474.
[10] Ego B, Grimsdale AC, Uckert F, Yu G, Srdanov G, Müllen K. Adv Mater 2002;14:809.
[11] Shu CF, Dodda R, Wu FI, Liu MS, Jen AKY. Macromolecules 2003; 36:6698.
[12] Shi JM, Zheng SY. Macromolecules 2001;34:6571.
[13] Lee YZ, Chen X, Chen SA, Wei PK, Fann WS. J Am Chem Soc 2001; 123:2296.
[14] Zheng M, Ding L, Gurel EE, Lahti PM, Karasz FE. Macromolecules 2001;34:4124.
[15] Bao Z, Peng Z, Galvin ME. Adv Mater 1998;10:680.
[16] Li XC, Liu Y, Liu MS, Jen AKY. Chem Mater 1999;11:1568.
[17] Chung SJ, Kwon KY, Lee SW, Jin JI, Lee CH, Lee CE, et al. Adv Mater 1998;10:1112.
[18] Pu YJ, Soma M, Tsuchida E, Nishide H. J Polym Sci, Part A: Polym Chem 2000;38:4119.
[19] Pu YJ, Soma M, Kido J, Nishide H. Chem Mater 2001;13:3817.
[20] Pu YJ, Soma M, Nishide H, Shirai S, Kido J. Jpn J Appl Phys 2002;41: 362.
[21] Pu YJ, Kurata T, Soma M, Kido J, Nishide H. Synth Met 2004;143: 207.
[22] Wang B, Wasielewski MR. J Am Chem Soc 1997;119:12.
[23] Pfeiffer S, Hörhold HH. Macromol Chem Phys 1999;200:1870.
[24] Moratti SC, Cervini R, Holmes AB, Baigent DR, Friend RH, Greenham NC, et al. Synth Met 1995;71:2117.
[25] Martinez-Ruiz P, Behnisch B, Schweikart KH, Hanack M, Luer L, Oelkrug D. Chem Eur J 2000;6:1294.
[26] Pommerehne J, Vestweber H, Guss W, Mahrt RF, Bassler H, Porsch M, Daub J. Adv Mater 1995;7:551.
[27] Leeuw DM, Simenon MMJ, Brown AR, Einerhand REF. Synth Met 1997;87:53.
[28] Suh MC, Chin BD, Kim MH, Kang TM, Lee ST. Adv Mater 2003;15: 1254.